

# Dynamic threshold adjustment in a proximity-based location tracking system using reference modules

Gel Han

Technische Universität München  
Boltzmannstraße 3  
D-85748 Garching b. München  
Email: hang@in.tum.de

Gudrun J. Klinker

Technische Universität München  
Boltzmannstraße 3  
D-85748 Garching b. München  
Email: klinker@in.tum.de

**Abstract**—In recent years, location tracking systems have become important in areas such as transportation, shopping, logistics and medicine. One of the most recent approaches are proximity-based location tracking systems, which use the received signal strength (RSSI) measured between a sender and an anchor module. The advantages of these systems are high scalability, minimal calibration effort and low costs. However, there are also disadvantages e.g. the fluctuating signal strength under certain circumstances in the environment. To detect, if an object has entered a predefined region, the RSSI must exceed a specified threshold. When the current signal fluctuates due to obstacles (other objects, people, etc.) the static threshold does not apply for the defined region any longer. In this case automatic adjustments of the threshold are made with the help of a reference module. Various factors are measured between reference, anchor as well as a sender module and subsequently used to correct the static threshold. The dynamic adjustment was tested through three experiments and showed satisfactory results concerning the hypotheses. For further research, additional factors might need to be included to make the proposed method more dynamic and responsive to the environment.

**Keywords**—Bluetooth, Bluetooth Low Energy, Correlation, Correlation Coefficient, Dynamic, Kalman Filter, Location, Location Tracking, Path Loss Exponent, Proximity, Received Signal Strength, Reference Module, RSSI, Signal Strength Fluctuation, Threshold, Tracking.

## I. INTRODUCTION

Proximity-based location tracking systems are becoming more and more popular and as a result are used more commonly because of a cost-benefit advantage over other methods/systems. The required hardware is available off-the-shelf and in comparison to other location tracking systems, they allow for an easier setup and higher scalability in terms of maintenance effort at lower costs. However, the systems also come with a disadvantage: The level of accuracy that can be reached with, for example, trilateration is higher than when using proximity. Companies like Apple are trying to bring proximity-based systems to the masses by providing suitable interfaces for hardware manufacturers.

Technologies like ZigBee and as of late also Bluetooth fulfill requirements for the use in a proximity-based location

tracking system. There are also systems on the market which include additional sensors to detect motion and which were specifically developed for localization purposes.

Usually, signal strengths measured from a receiver module, also called the anchor, to a sender module are compared to a static value (also referred to as threshold in the following). Depending on the difference of the respective signal strengths, the location tracking system moves to a specific state. If the signal strength is higher than the static value, the system concludes that the sender module is positioned inside a certain region and if it is lower, it is outside of this region. These static values are often stored in the anchors themselves or in a database on a computer in the backend. If there are two values saved indicating "far away" (low value) and "nearby" (high value), then matching the current signal strength against these two values reveals in which range the user/the sender module could be.

One problem though with wireless technologies like Bluetooth is the fluctuation of the signals over time even while receiver and sender are placed at fixed locations. Environmental influences, multipath effects and shadowing lead to such fluctuations [1], making it more difficult as well as unstable to compare against specific static values. If the current signal strength values increase because of fluctuations while the threshold stays the same because only one is measured in an initialization step, the region defined by the threshold increases.

This paper investigates the idea that instead of static values, we could use dynamic values which adjust themselves automatically through periodic measurements. The system would always obtain the regions defined by exactly those dynamic values. One way to achieve this is to place a reference module at a fixed spot, let an anchor measure the signal strength of the reference module in periodic intervals and see if any fluctuations can be detected (see figure 1). If they can be detected and if they correlate with other sender modules, the static values could be adjusted. In the case of positive fluctuations, the values increase. In the case of negative fluctuations, they decrease.

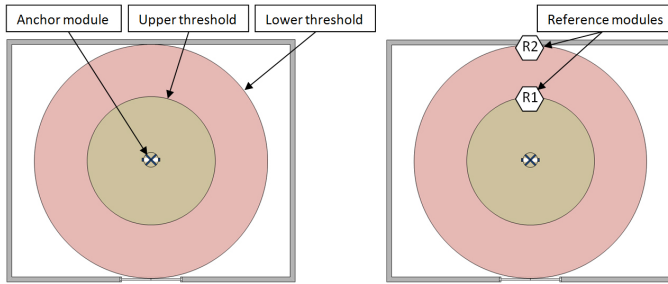


Fig. 1. On the left: Initial setup with an anchor module mounted on the ceiling in the center of the room. Two threshold values (one for “nearby”/upper threshold and one for “far away”/lower threshold) from previous measurements are stored on a computer used for the calculation of the location. On the right: The proposed setup with two reference modules mounted on the ceiling in specific ranges for defining the two regions.

To show that reference modules can be used to improve the stability of a proximity-based location tracking system, some hypotheses are necessary:

- Hypothesis 1: Reference module 1 (R1) records fluctuations caused by environmental influences, multipath effects and shadowing
- Hypothesis 2: The fluctuations recorded by R1 are comparable to the fluctuations recorded by another sender module (S1)
- Hypothesis 3: Through the measured signal strength of R1, the static value depicting the region can be adjusted to stay similar despite fluctuations

## II. RELATED WORK

Goldsmith et al. [2] published a book about various wireless technologies (including Bluetooth) describing the RSSI-distance relation as well as several propagation effects on the signal power. For an in-depth analysis of location-based services and applications focusing on WiFi, see [3].

Patwari et al. [4] used a proximity-based location tracking system to analyze with the Cramér-Rao bound on what an unbiased real time location tracking system (RTLS) without channel fading and multipath effects would look like. They mention that a more precise location tracking system implies higher costs, overall bigger devices and increased power consumption. Those are the reasons why they continued with a simple proximity-based system based on received signal strength measurements. Kim et al. [5] and Mechitov et al. [6] also use a proximity-based location tracking system but with an anchor grid to estimate the target’s position. They try to use more sensors to increase stability as well as accuracy by using anchors as reference modules.

Dil et al. [7] show that range/proximity-based location tracking systems perform better with less calibration effort than a system based on RSSI fingerprints. Proximity-based systems have the advantage of a fast setup and less calibration effort. Erceg et al. [8] and Solahuddin et al. [9] worked on the Log Normal Shadowing model which calculates the path loss of a signal over a certain distance. We use this model because of

its accurate estimations which furthermore takes effects such as multipath and shadowing into account. The Log Normal Shadowing model can also be used to calculate the Path Loss Exponents of various test setups when the signal strengths are known. These values give us more information about the test environment.

Cinefra et al. [10] present in their work that the orientation of anchors when placing them is important. They point out that Gaussian and Kalman filters yield the best results when applied to the raw signal strength values. They also use an adaptive system where a base station (one of the anchors) constantly updates the used path loss model with new calibration parameters to calculate a new position for the user. Cinefra et al. determined the following parameters to have a negative effect on location tracking accuracy: various sender devices having varying levels of transmitting power, the height of the sender devices and people’s presence when tracking the sender modules. However, they were not able to analyze and prove any effects in detail.

Turner et al. [11] use a self-calibrating location tracking system based on WiFi. They collect fingerprints from access points on known positions and use them for calibrating the new environment for the system. They conclude that when using 802.11 access points, it is unrealistic to set up a location tracking system with an accuracy better than five meters due to environmental as well as algorithmic issues.

Two papers by Pan et al. [12] [13] describe how to transfer a calibrated environment from space A to space B with a minimized amount of calibration effort. This is useful to show how two different, independent spaces are related to each other since multiple similar factors are identified with a quadratically constrained quadratic program (QCQP). They analyzed transferring calibrated and collected information across space, time and devices.

## III. MATERIAL AND METHODS

In our system, we use Bluetooth modules from the company connectBlue to set up a state-of-the-art proximity-based location tracking system. We use the Bluetooth module OBS421 as anchor and several OLS425 modules as sender modules. There are some limitations such as hardware restrictions when relying on these off-the-shelf products but the low costs of the modules outweighed the disadvantages.

The general setup of the system is as follows: the sender modules need to advertise an ID in a periodic time interval while the anchor module needs to scan the area for all Bluetooth modules and then measure the signal strength for each of the found modules. The anchor module is connected to a computer in the backend which logs all the measured data, e.g. signal strengths, into a database.

The sender modules send an advertisement with their ID every 250 milliseconds and the anchors scan the environment every 1.28 seconds. Due to the Bluetooth specifications and the hardware restrictions, it is not possible to scan without modifying the firmware to operate at a higher rate. In order to find the tags periodically, we chose 250 milliseconds based

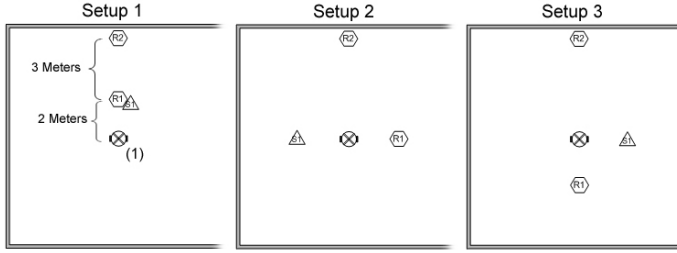


Fig. 2. Overview of the three different setups with the location tracking anchor (1), the two reference modules R1, R2 as well as the sender module S1 placed at their respective positions. R1 and S1 were always placed 2 meters apart from the anchor. R2 was 5 meters apart.

on [14] for a good balance between power consumption and finding the tags at all times. Additionally, we went with the lowest possible interval of 1.28 seconds to scan for new tags for a high update rate. A test software was written to conduct experiments in an office with the size of approx. 10x10x3 meters. Three different setups were tested (see figure 2). The reference module R1 was placed 2 meters next to the anchor at the ceiling. The second reference module R2 was placed 5 meters next to the anchor (see figure 3). As part of each test run, there were time spans where either people were in the office moving around causing fluctuations or the office was empty.

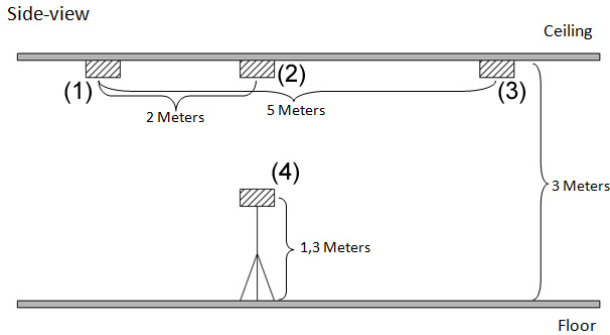


Fig. 3. Side view of setup 1 with the location tracking anchor (1), module R1 (2), module R2 (3) and module S1 (4). S1 was mounted on a tripod. The other modules were attached to the ceiling with tape.

Since the receiver and sender modules use different antennas, the orientation of the modules has to be taken into account when planning the experiments. The antenna plots of the receiver module [15] show a uniformly distributed characteristic but the plot for the sender module shows that the antenna scatters more towards one direction (see figure 4).

We used Pearson's R correlation coefficient to obtain some sort of information about the correlation between the data of each module. The correlations for each setup can be seen in table I. Analyzing the results after conducting three test runs, we found that only setup 1 was interesting to further investigate. The only noteworthy correlation was recorded in setup 1, where S1 was placed underneath R1. In all the other tests, the correlation was not significantly high suggesting

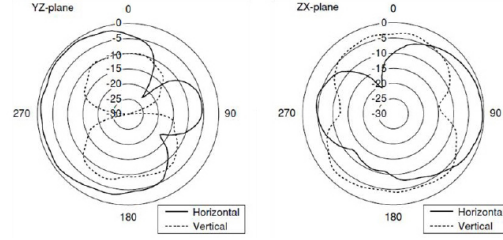


Fig. 4. Antenna characteristics of the sender module. In (1) the directivity of the antenna can be seen on the left graph. Because of the directivity, the sender modules have to be installed in a specific orientation on the ceiling.

that two modules share a similar trend regarding the signal strengths. Therefore, we repeated the tests with setup 1 two more times for a total of three test runs (see table II for T2 and T3).

In all test runs for setup 1, the modules were positioned in the exact same locations on the ceiling. Every experiment began in the afternoon and continued over night to specify whether the results showed significant differences when people were moving in the office or when the office was empty at night. For each of the located sender modules, four different values were stored in the database: the signal strength, the moving average of the signal strength, the standard deviation of the signal strength as well as the estimated Kalman filter value up to now. After storing the signal strength values, there were two options to adjust the threshold dynamically.

- Option 1: Calculate the moving average as well as the standard deviation from the stored signal strength values up to now and depending on the later, the threshold is adjusted (increased or decreased).
- Option 2: Use the standard deviation of the estimated Kalman filter value to decide if the threshold should be adjusted or not.

Figure 5 shows how the dynamic adjustments of the thresholds work. Let  $x_1$  be the raw signal for R1 and  $x_2$  the raw signal for S1.  $f(x)$  is the filter which is applied to the raw signal (moving average, Kalman, ...) and  $g(x)$  is the current standard deviation for all the previous signal strength values.  $h(x_1, x_2)$  calculates  $\beta$ , the correlation coefficient. The threshold is depicted as  $y$ .  $m_1$  and  $m_2$  are the current moving average values of R1 and S1. The query on the raw signal strengths can be seen in algorithm 1. For the experiments,  $\alpha$  was set to 0.5 for the first test run and then 0.3 for the later ones.  $\gamma$  was always set to 0.5.

#### Algorithm 1 adjust threshold

```

if  $h(x_1, x_2) > \gamma \wedge g(f(x_1)) > \alpha \wedge g(f(x_2)) > \alpha \wedge$ 
 $(|f(x_1) - m_1| > 0 \wedge |f(x_2) - m_2| > 0) \vee$ 
 $(|f(x_1) - m_1| < 0 \wedge |f(x_2) - m_2| < 0)$  then
   $y = y + \frac{(m_1 - f(x_1)) + (m_2 - f(x_2))}{2}$ 
end if

```

First, the algorithm examines if the correlation coefficient is greater than  $\gamma$ . Additionally, the standard deviations of both

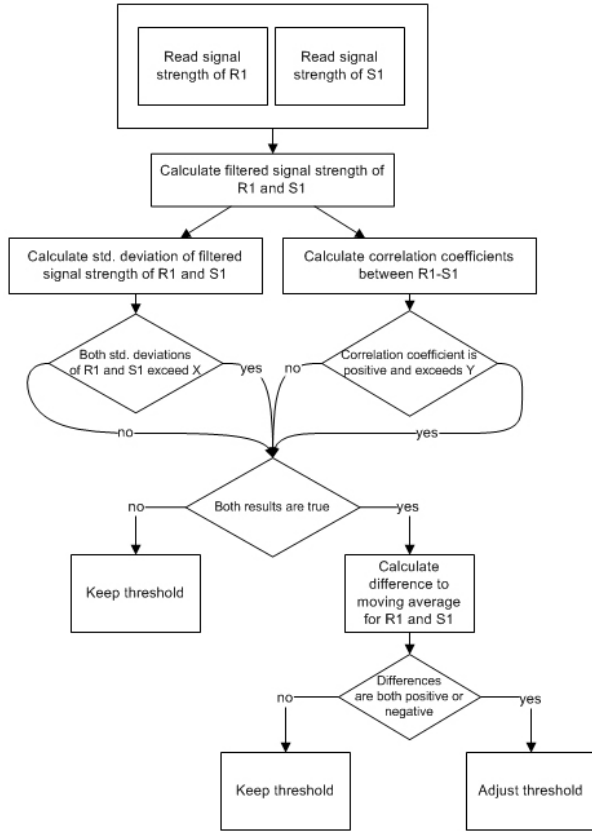


Fig. 5. The process behind the dynamic threshold adjustment. The raw signal strengths of R1/R2 and S1 are the inputs while the output decides whether the threshold should be adjusted or not.

signals from R1 and S1 are calculated to check the fluctuations in the data. In the last part of the query, the absolute difference between the moving average and the filtered signal strength value is calculated for each module. If the differences are either both positive or both negative and the rest of the factors are true, then the threshold  $y$  is adjusted. The adjustment is based on the mean value of added differences from both modules.

Since the distances between the modules in the test setup could be measured, we were able to calculate the expected signal strengths via the Log Distance Path Loss model (also called Log Normal Shadowing model):

$$P_d = P_{d0} - 10 * n * \log_{10}\left(\frac{d}{d_0}\right) + \chi$$

The Log Distance Path Loss model describes the estimated signal strength at a given distance and includes factors such as a reference signal strength value or the Path Loss Exponent (PLE). The Path Loss Exponent represents the signal drop over distance in various environments. Calculating the PLE value of each module and comparing them would provide insight into the influences (people, objects obstructing the line of sight etc.) in a test environment if the values would be significantly different (see [16]).

$P_d$  and  $P_{d0}$  represent signal strengths at given distances with

$d_0$  being a fixed distance (usually 1 meter).  $P_{d0}$  serves as signal strength reference which has to be measured beforehand.  $n$  is the Path Loss Exponent. In general,  $n = 2$  is used for free space while higher values are used to model more obstacles in the environment and lower values for an unobstructed line of sight between the modules.  $\chi$  is a zero-mean normally distributed value which describes the shadowing effect:

$$\chi_\sigma \sim N(0, \sigma^2)$$

#### IV. RESULTS

The correlation was checked between modules and calculated for the following combinations:

- Reference module 1 (R1) - Reference module 2 (R2)
- Reference module 2 (R2) - Sender module 1 (S1)
- Reference module 1 (R1) - Sender module 1 (S1)

The results can be seen in table I. A value between +1 and 0 represents a positive correlation whereas a value between 0 and -1 indicates a negative correlation (and 0 for no correlation).

TABLE I  
CORRELATION BETWEEN THE MODULES FOR EACH SETUP.

Setup 1 Test run 1 (T1)	Raw	Moving average	Kalman
R1 and R2	0.19	0.25	0.23
R2 and S1	-0.04	-0.15	-0.05
R1 and S1	0.08	0.46	0.11

Setup 2 Test run 1 (T1)	Raw	Moving average	Kalman
R1 and R2	0.20	0.77	0.24
R2 and S1	0.0	-0.20	0.0
R1 and S1	-0.12	-0.58	-0.16

Setup 3 Test run 1 (T1)	Raw	Moving average	Kalman
R1 and R2	-0.52	-0.93	-0.54
R2 and S1	0.09	-0.13	0.09
R1 and S1	-0.28	-0.09	-0.29

A positive correlation between R1 and R2 as well as R1 and S1 can be seen in the first two test runs. The same goes for the first two test runs for R2 and S1 with negative correlations. Setup 1 was the only test run with a positive correlation between R1 and S1. If we take the moving average and calculate all coefficients with the current signals for each tag, the correlations become more apparent (see table I). The gray rows depict the values with correlations greater than 0. We decided to conduct two more test runs with setup 1 since it was showing promising results regarding the correlation of R1-S1. The results of T2 and T3 can be seen in table II. In the following, we are only discussing the three tests (T1, T2 and T3) of setup 1.

As for taking the reference modules as thresholds: The minimum value of T1-R1 was -75 and the maximum value of T1-R2 was -73. Assuming that we take the value of R1 as dynamically changing upper threshold and R2 as dynamically changing lower threshold, it would have been problematic if these values were read continuously since the lower threshold

would be higher than the upper threshold. However, there was no entry of R1 measuring the value -75 and R2 measuring the value -73 at the same time in the recorded data.

For the second test run, the minimum value of R1 was -77 and the maximum value of R2 was -83. Looking at the data, there was no overlap of the values from R1 and R2 so taking the values from R1 as upper threshold and the values from R2 as lower threshold seems unproblematic. It is remarkable that the signal from T2-R2 is considerably lower than the signal from T1-R2. This can be explained by a slight correction of the module placement after test run 1. The minimum value of R1 (-74) in test run 3 and the maximum value of R2 (-83) do not overlap either and therefore can be used as upper threshold and lower threshold respectively.

The means for T1 to T3 were taken as initial thresholds and were then adjusted with the averaged difference between the moving average and the estimated Kalman value of the respective test runs.

TABLE II  
SUMMARY OF ALL MEANS, STANDARD DEVIATIONS AND CALCULATED PATH LOSS EXPONENTS FOR EACH MODULE AND TEST RUN.

Setup 1 Test run 2 (T2)	Raw	Moving average	Kalman
R1 and R2	0.33	0.32	0.37
R2 and S1	-0.25	-0.12	-0.27
R1 and S1	0.08	0.36	0.16

Setup 1 Test run 3 (T3)	Raw	Moving average	Kalman
R1 and R2	0.07	0.75	0.17
R2 and S1	-0.12	-0.83	-0.15
R1 and S1	-0.18	-0.64	-0.19

Test run 1 (T1)	R1	R2	S1
Mean	-71.84	-77.92	-79.17
Standard deviation	0.49	1.17	1.28
PLE $n$	1.54	1.46	2.74

Test run 2 (T2)	R1	R2	S1
Mean	-75.42	-92.90	-81.09
Standard deviation	0.71	1.67	0.72
PLE $n$	2.65	3.59	3.26

Test run 3 (T3)	R1	R2	S1
Mean	-71.09	-90.06	-91.71
Standard deviation	0.47	2.11	6.59
PLE $n$	1.3	3.18	5.68

Table II shows all the mean and standard deviation values of the test runs with the Path Loss Exponents describing how people, shadowing, multipath effects and other influences led to a decrease in signal strength during the tests. A person moving the tripod with the module S1 explains why the Path Loss Exponent value was so surprisingly high at T3-S1.

A summary of the amount of threshold adjustments in all three test runs:

- T1: 4459 adjustments out of 9900 signal values
- T2: 264 adjustments out of 670 signal values
- T3: 1078 adjustments out of 26000 signal values

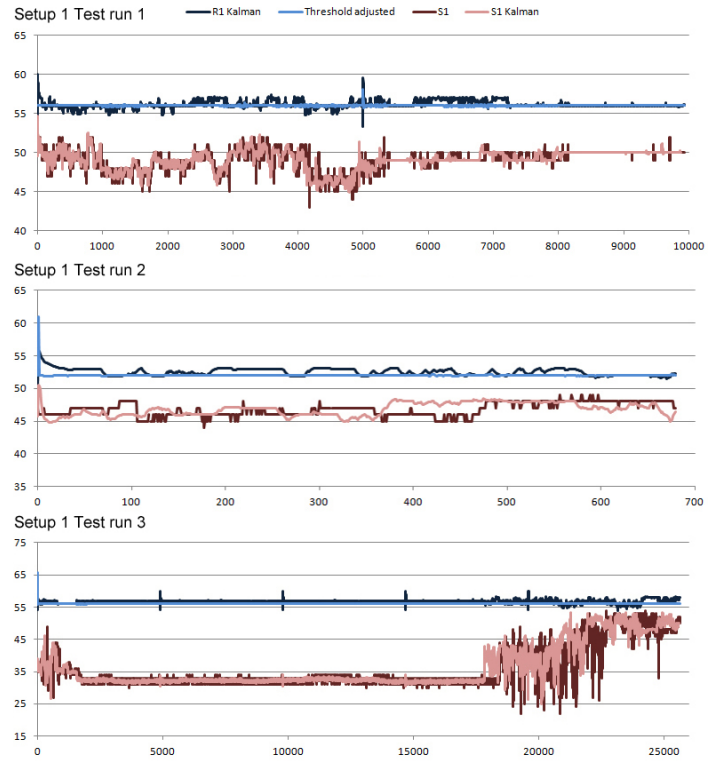


Fig. 6. The results from each test run visualized with the adjusted threshold drawn in lightblue. The raw signal strength values were recorded with an offset of +128 dbm. The values seen in the figure are the filtered/adjusted ones. An adjustment of the threshold can be seen e.g. in the first test run at timestamp 5000.

## V. DISCUSSION

The results from table I show only positive correlations for the signal measurements where S1 is placed underneath R1. This suggests that the same could happen when S1 is placed underneath R1 in setup 2 and 3. These cases need to be examined in future work.

The first hypothesis can be proven with all test runs for setup 1 (see figure 6). In the first two graphs, fluctuations of the signal strengths can be seen at the beginning when people were still in the office. Then the signal stabilizes while on the third graph, toward the end, people were entering the office and moving the tripod (S1).

The second hypothesis can be proven with the test runs T1 and T2 (the correlation coefficients for raw signals as well as filtered signals are positive).

The third hypothesis can be proven with all test runs since none of the adjusted thresholds overlapped during the experiments. For the first test run, the signal peak in the middle was recorded on both modules, R1 and S1, and the correlation was positive at that point which caused the threshold adjustment. For the third test run, the correlation at the end was not positive for both modules. Therefore, the threshold was not adjusted for the rest of the test run.

For now, the only adjustment made to the threshold was to either add or subtract the difference of the moving average and the filtered signal. Adjustments were only made if the standard deviations crossed a certain value which, for now, was static in most cases (0.5).

Furthermore, an initial static value has to be measured and inserted in the current system. This is done by taking the mean of a measurement which usually contains at least 500 signal values. Instead of taking a static value (the mean), the live signal value of R1 can be used. Considering the data from test run 1 and 2, this would work fine as both signal values from R1 and S1 would always be apart with enough distance between each other. Only the third test run would prove to be problematic since both adjusted and filtered values would converge and be apart for 2.5 dbm.

A more thorough examination of the correlation between the modules at different locations and various test environments has to be done to specify if the threshold adjustment would also work under difficult conditions.

The Path Loss Exponent values in table II were similar for the first and second test run while the third test included higher values due to changes in the environment and the movement of S1 itself. In addition to the factors in our proposed method, a change in the Path Loss Exponent could also be included in the query to make the system more responsive. The current signal strength of R1 could be used as a reference signal strength and R2 could be measured for the expected signal strength at the known distance  $d$  to calculate the PLE. The correlations between R1 and R2 were not significantly high in our tests but this needs to be examined in further experiments with the modules placed at various positions. An example of including the updated PLE value when calculating the user's position can be seen in [17].

## VI. CONCLUSION

Test runs show that signal strength fluctuations can be detected by using reference modules which are located at fixed places on the ceiling. Additionally, two reference modules which are positioned at different locations show no relation to each other.

A positive correlation between the data of a reference module on the ceiling and the data of a sender module positioned underneath it can be seen in the results. This indicates that for future work, more reference modules have to be placed around the anchor to detect any correlation when the sender module is moving.

The requirement was to set up a simple location tracking system with room-level accuracy. The proposed system would cost a maximum of \$500 per room. At this price, the hardware would come with disadvantages and restrictions which we try to compensate by using extra reference modules to have stable thresholds with a fluctuating signal.

The proposed method to detect and adjust thresholds was tested successfully on a state-of-the-art proximity-based lo-

cation tracking system. The results suggest that the location tracking system would react better to fluctuations compared to the system without any adjustments but this has to be investigated more thoroughly. In addition to that, more factors such as the current Path Loss Exponent value should be evaluated and included to make the system more responsive to various environments.

## REFERENCES

- [1] A. Neskovic, N. Neskovic, and G. Paunovic, "Modern approaches in modeling of mobile radio systems propagation environment," *Communications Surveys Tutorials, IEEE*, vol. 3, no. 3, pp. 2–12, Third 2000.
- [2] A. Goldsmith, *Wireless Communications*. New York, NY, USA: Cambridge University Press, 2005.
- [3] A. Kushki, K. Plataniotis, and A. Venetsanopoulos, *WLAN Positioning Systems: Principles and Applications in Location-Based Services*, ser. WLAN Positioning Systems: Principles and Applications in Location-based Services. Cambridge University Press, 2012. [Online]. Available: <http://books.google.de/books?id=8TANplmj2PUC>
- [4] N. Patwari and A. O. Hero, III, "Using Proximity and Quantized RSS for Sensor Localization in Wireless Networks," in *Proceedings of the 2Nd ACM International Conference on Wireless Sensor Networks and Applications*, ser. WSN '03. New York, NY, USA: ACM, 2003, pp. 20–29. [Online]. Available: <http://doi.acm.org/10.1145/941350.941354>
- [5] W. Kim, K. Mechitov, J.-Y. Choi, and S. Ham, "On target tracking with binary proximity sensors," in *Information Processing in Sensor Networks, 2005. IPSN 2005. Fourth International Symposium on*, April 2005, pp. 301–308.
- [6] K. Mechitov, S. Sundresh, Y. Kwon, and G. Agha, "Poster Abstract: Cooperative Tracking with Binary-detection Sensor Networks," in *Proceedings of the 1st International Conference on Embedded Networked Sensor Systems*, ser. SenSys '03. New York, NY, USA: ACM, 2003, pp. 332–333. [Online]. Available: <http://doi.acm.org/10.1145/958491.958546>
- [7] B. Dil and P. Havinga, "On the calibration and performance of RSS-based localization methods," in *Internet of Things (IOT), 2010*, Nov 2010, pp. 1–8.
- [8] V. Erceg, L. Greenstein, S. Tjandra, S. Parkoff, A. Gupta, B. Kulic, A. Julius, and R. Bianchi, "An empirically based path loss model for wireless channels in suburban environments," *Selected Areas in Communications, IEEE Journal on*, vol. 17, no. 7, pp. 1205–1211, Jul 1999.
- [9] Y. Solahuddin and R. Mardeni, "Indoor empirical path loss prediction model for 2.4 GHz 802.11n network," in *Control System, Computing and Engineering (ICCSCE), 2011 IEEE International Conference on*, Nov 2011, pp. 12–17.
- [10] N. Cinefra, "An adaptive indoor positioning system based on Bluetooth Low Energy RSSI," 2013.
- [11] D. Turner, S. Savage, and A. Snoeren, "On the empirical performance of self-calibrating WiFi location systems," in *Local Computer Networks (LCN), 2011 IEEE 36th Conference on*, Oct 2011, pp. 76–84.
- [12] S. J. Pan, V. W. Zheng, Q. Yang, and D. H. Hu, "Transfer Learning for WiFi-based Indoor Localization," pp. 43–48, 2008.
- [13] S. J. Pan, D. Shen, Q. Yang, and J. T. Kwok, "Transferring Localization Models Across Space Transfer Learning for WiFi Localization," 2008.
- [14] R. Heydon, *Bluetooth Low Energy: The Developer's Handbook*, ser. Pearson Always Learning. Prentice Hall, 2012. [Online]. Available: <http://books.google.de/books?id=Ag2tXwAACAAJ>
- [15] Fractus, "Fractus Compact Reach Xtend Bluetooth, Zigbee, 802.11 b/g/n WLAN Chip Antenna," [http://www.fractus.com/sales\\_documents/FR05-S1-N-0-102/UM\\_FR05-S1-N\\_0-102.pdf](http://www.fractus.com/sales_documents/FR05-S1-N-0-102/UM_FR05-S1-N_0-102.pdf), p. 5, [Online; accessed 10-January-2015].
- [16] J. Miranda, R. Abrishambaf, T. Gomes, P. Goncalves, J. Cabral, A. Tavares, and J. Monteiro, "Path loss exponent analysis in Wireless Sensor Networks: Experimental evaluation," in *Industrial Informatics (INDIN), 2013 11th IEEE International Conference on*, July 2013, pp. 54–58.
- [17] A. Golestani, N. Petreska, D. Wilfert, and C. Zimmer, "Improving the precision of RSSI-based low-energy localization using path loss exponent estimation," in *Positioning, Navigation and Communication (WPNC), 2014 11th Workshop on*, March 2014, pp. 1–6.